

Transform your Digital Camera into a Flatbed Scanner

Paper Id: 794

Abstract. We propose to extend the use of a digital camera to a new application, which consists basically in transforming it into a flatbed scanner. Our approach consists in simulating the flattening of warped documents, by means of computer vision techniques. In particular, with regard to the digitization of a book, we show that the drawbacks related to the use of a scanner can be bypassed. The corrections of some or all geometric and photometric distortions appearing in the image of an opened book, including perspective transformations, are discussed and compared, regarding two different techniques of shape from X, namely shape from shading and shape from contour. The performances of the proposed techniques are illustrated by experiments on real images.

1 Introduction

The digitization of documents currently undergoes considerable expansion as a consequence of the possibilities of remote consultations via the Internet. The traditional digitization process, by means of a flatbed scanner, has two drawbacks with regard to the digitization of a book. Repetitive handling, consisting in turning a page and then pressing the book to force it flat, is quite tedious. In addition, some defects will appear on the digitized image: blurred or deformed characters, effects of parallax, shaded tones for a uniformly white sheet. To compensate for these two weaknesses, a lot of dedicated systems have been developed, but of course, in such cases, it cannot be referred to as a consumer product. An alternative consists in simulating the flattening of warped documents, by means of computer vision techniques, where the scanner, whose optical system is difficult to modelize, is replaced by a numerical reflex camera. Our work is set up within this framework. To simulate a corrected image in conformity with the geometric and photometric modelings, it is necessary to calculate the shape of the document, starting from the initial image (*cf.* Figure 1a), then to use this shape to simulate the image of the flattened document. The remainder of this

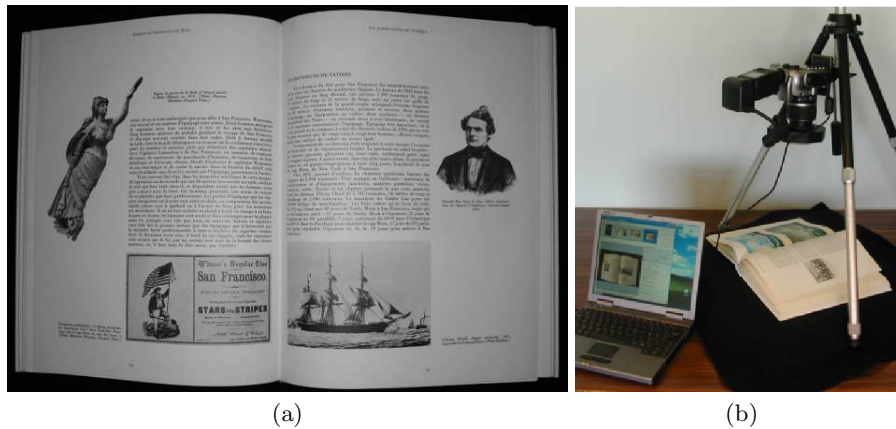


Fig. 1. (a) Photograph of an opened book taken as input of our processing chain and (b) optical bench.

paper is as follows: Sections 2 and 3 overview the geometric and photometric corrections; Section 4 compares two different approaches; Section 5 concludes our contribution.

2 Geometric Correction

2.1 Previous Work

2D-2D Methods. A very simple geometric correction applied on images of warped documents has been proposed in [1]: the orientation of characters near the binding is evaluated, in order to rotate them and make them horizontal. The results are rather disappointing. As said in [2], “Image processing algorithms cannot, without a priori information, determine document shape, which is necessary to solve the restoration problem”. In [3], a judicious 2D-2D deformation is introduced, considering that the boundary of each page must become a rectangle: the results are nice, but a “paper checkerboard pattern” has to be placed behind the document, thus giving some 3D information. All other methods require a 3D model of the document, as shown in Figure 2. Several techniques of “shape from X” (SFX) have been proposed.

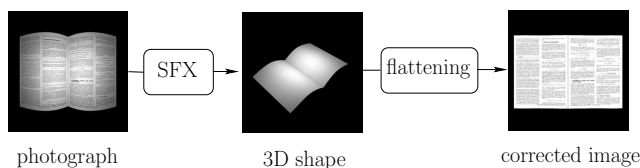


Fig. 2. 2D-3D-2D methods of geometric correction.

2D-3D-2D Methods. In order to compute the 3D shape of a document, some authors need more than one image. In [4], two images are taken under two angles of view, while in [5], the two images are taken with two different lighting systems. In both cases, a precise calibration (geometric for [4] and photometric for [5]) is required. In [2], a structured-lighting system is used and several images are needed to get the 3D shape. This last technique, which had originally been proposed in [6], is rather destined to cultural heritage digitization, because of the very expensive equipment required.

Other techniques need a single image. In [7], the deformations of the lines of text are analyzed, which provides rather good results. Another technique, proposed in [8], analyzes the contours of the pages. These two last techniques are similar, because they both suppose that these lines are horizontal on the unwarped document. Finally, shape from shading has been used, originally on flatbed scanned images [9], and more recently on photographs [5, 10, 11]. To our knowledge, nobody has used, as this could have been done in [1], the orientation of the characters to compute the 3D shape of the document.

If a variety of SFX techniques has been used, the second stage of the 2D-3D-2D methods *i.e.*, flattening, is most of the time the same. In fact, as soon as the 3D document is a ruled-developpable (or cylindrical) surface, it is easy to

unwarp it (see for example [10, 4, 8]). Moreover, let us mention the physics-based technique proposed in [2], which is well adapted to the case of non-cylindrical documents.

Finally, unwarp the document moves the pixels in such a way that they don't coincide with a regular grid anymore. As a consequence, an interpolation step is needed, in order to produce the corrected image. Some authors [5] have implemented specific interpolation methods, while the others generally use the well-known Smythe's algorithm [12].

2.2 Our Contribution

In this paper, we address shape from contour (SFC) and shape from shading (SFS), since these two techniques need only one image and, as we will see further, a rigorous calibration is not always needed to make them work well.

Perspective Camera Model. We use a digital camera (Canon EOS 300D, 6.1Mp) fixed on an optical bench (*cf.* Figure 1b) and piloted via a computer. The lighting system is an annular flash (Sigma EM-140 DG). In order to minimize the blur, the objective is as closed as possible. As we can see in Figure 3, the projection model is a pinhole model, whose center point is the optical center C . The 3D-coordinate object system ($C\mathbf{xyz}$) coincides with that of the camera. We note ($A\mathbf{ij}$) the two-dimensional system used in the image plane. We introduce the calibration matrix (*cf.* [13], page 156):

$$\mathbf{K} = \begin{pmatrix} f & s & i_o \\ 0 & \tau f & j_o \\ 0 & 0 & 1 \end{pmatrix}, \quad (1)$$

where f is the focal length (expressed in the x -axis unit); (i_o, j_o) are the coordinates of the principal point O ; τ and s denote, respectively, the ‘‘scale factor’’ and the ‘‘obliquity factor’’ of the pixels. For a pixel Q of coordinates (i, j) in system ($A\mathbf{ij}$), the conjugate object point is a point P whose coordinates are (x, y, z) in system ($C\mathbf{xyz}$). The unknown of the problem is function u such that the surface of the document is represented by the equation:

$$z = u(i, j). \quad (2)$$

In Figure 3, another plane, denoted Π , has been represented. This is the plane on which the document will be unwarped. This plane could be chosen arbitrarily at any distance d from C . But, since we suppose moreover that the binding of the book is orthogonal to the optical axis (‘‘fronto-parallel’’ hypothesis, denoted as H1 in the sequel), it is convenient to choose Π so that it contains the binding.

Shape From Contour. On the one hand, the perspective projection equation, mapping the object coordinates $\mathbf{P} = (xyz)^T$ of P to the pixel coordinates $\mathbf{Q} = (ij)^T$ of its projection Q , simplifies to (*cf.* [13], page 155):

$$z \begin{pmatrix} \mathbf{Q} \\ 1 \end{pmatrix} = \mathbf{K} (\mathbf{I}_3 | \mathbf{O}_3) \begin{pmatrix} \mathbf{P} \\ 1 \end{pmatrix} = \mathbf{KP}, \quad (3)$$

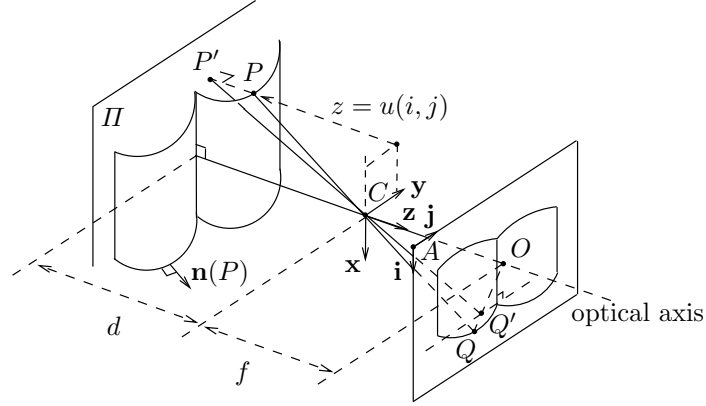


Fig. 3. Perspective projection and weak perspective projection.

where \mathbf{I}_3 represents the order-3 unit matrix and \mathbf{O}_3 the null vector of dimension 3. In addition, the equation of weak perspective projection, which binds the orthogonal projection P' of P on Π to its conjugate point Q' in the image, of coordinates $\mathbf{Q}' = (i' j')^T$, is written (*cf.* [13], page 171):

$$\begin{aligned} -d \begin{pmatrix} \mathbf{Q}' \\ 1 \end{pmatrix} &= \mathbf{K} \begin{pmatrix} 1 & 0 & 0 & 0 \\ 0 & 1 & 0 & 0 \\ 0 & 0 & 0 & -d \end{pmatrix} \begin{pmatrix} \mathbf{P} \\ 1 \end{pmatrix} \\ &= \mathbf{K} \begin{pmatrix} 1 & 0 & 0 \\ 0 & 1 & 0 \\ 0 & 0 & 0 \end{pmatrix} \mathbf{P} - d \mathbf{K} \begin{pmatrix} 0 \\ 0 \\ 1 \end{pmatrix}. \end{aligned} \quad (4)$$

Deducing \mathbf{P} from (3), and deferring in (4), we obtain:

$$-d \begin{pmatrix} \mathbf{Q}' \\ 1 \end{pmatrix} = z \mathbf{K} \begin{pmatrix} 1 & 0 & 0 \\ 0 & 1 & 0 \\ 0 & 0 & 0 \end{pmatrix} \mathbf{K}^{-1} \begin{pmatrix} \mathbf{Q} \\ 1 \end{pmatrix} - d \begin{pmatrix} \mathbf{Q}_o \\ 1 \end{pmatrix}, \quad (5)$$

where $\mathbf{Q}_o = (i_o j_o)^T$ is the coordinate vector of the principal point. For any matrix \mathbf{K} of the form (1), it is easy to show that:

$$\mathbf{K} \begin{pmatrix} 1 & 0 & 0 \\ 0 & 1 & 0 \\ 0 & 0 & 0 \end{pmatrix} \mathbf{K}^{-1} = \begin{pmatrix} 1 & 0 & -i_o \\ 0 & 1 & -j_o \\ 0 & 0 & 0 \end{pmatrix}. \quad (6)$$

Consequently, the relation between \mathbf{Q} and \mathbf{Q}' , *i.e.*, between perspective and weak perspective projections, is written:

$$\frac{d}{z} \begin{pmatrix} \mathbf{Q}' \\ 1 \end{pmatrix} + \begin{pmatrix} \mathbf{Q} \\ 1 \end{pmatrix} = \left(\frac{d}{z} + 1 \right) \begin{pmatrix} \mathbf{Q}_o \\ 1 \end{pmatrix}. \quad (7)$$

From that we deduce the two equalities:

$$z = -d \frac{i' - i_o}{i - i_o} \quad ; \quad z = -d \frac{j' - j_o}{j - j_o}. \quad (8)$$

The double equality (8) corresponds to expressions of z which are more general than that given in [8], where the principal point is supposed to coincide with the origin A of the image system. Initially, let us notice that our analytical approach, which is opposed to the purely geometrical approach of [8], highlights the fact that the only intrinsic parameters used in (8) are the coordinates (i_o, j_o) of the principal point. Let us recall that d can be selected in an arbitrary way, which means that u can be calculated only up to a scale factor (*i.e.*, the surface can be reconstructed only up to a scale factor).

A second remark is that we can easily deduce, from (7), that the points Q and Q' define lines forming a bundle in the image, whose center is the principal point O (*cf.* Figure 4). Indeed, we know that any linear combination of the vectors $(\mathbf{Q}^T \mathbf{1})^T$ and $(\mathbf{Q}'^T \mathbf{1})^T$ represents a point in the image which is located on the line (QQ') . Since Q and Q' are the two image points of an unspecified point P in the scene, all the considered lines contain necessarily O .

Finally, let us notice that for a given pixel Q , the two equations (8) include three unknowns (i', j', z) if the coordinates (i_o, j_o) of the principal point are known, and five unknowns otherwise. In both cases, (8) is an under-constrained system. In a general way, there is no other equation binding these unknowns: the problem is ill-posed *i.e.*, we can not express the value of z associated to a pixel.

In order to render the problem well-posed, we must add several assumptions. A first assumption is that the surface of the document is a specific skew surface, that is a cylindrical surface, whose generators are parallel to the binding (assumption H2). For a pixel Q , denote Q_b and Q_t the pixels located at the intersections between the straight line passing by Q which is parallel to the binding B , and the contours C_b and C_t of the page (*cf.* Figure 4). Thanks to assumptions H1-H2, the three pixels Q , Q_b and Q_t are conjugate to scene points which have the same z . Cutting off the two equations of form (7) obtained for pixels Q_b and Q_t , we obtain the vectorial equality:

$$-\frac{d}{z} (\mathbf{Q}'_b - \mathbf{Q}'_t) = \mathbf{Q}_b - \mathbf{Q}_t, \quad (9)$$

which is equivalent to a system of two equations with five unknowns (the coordinates of pixels Q'_b and Q'_t , plus z). This last system becomes well-constrained thanks to a new hypothesis saying that the contour of the flattened page is rectangular (assumption H3). Knowing that the binding B is not changed by flattening, it rises from hypotheses H1-H2-H3 that the pixels of C_b are moved, by flattening, on the straight line L_b orthogonal to B which contains the lowest-pixel B_b of B . Similarly, the pixels of C_t are moved on the straight line L_t orthogonal to B which contains the highest pixel B_t of B (*cf.* Figure 4). If the coordinates of O are known, then it is enough to observe Figure 4 to note that

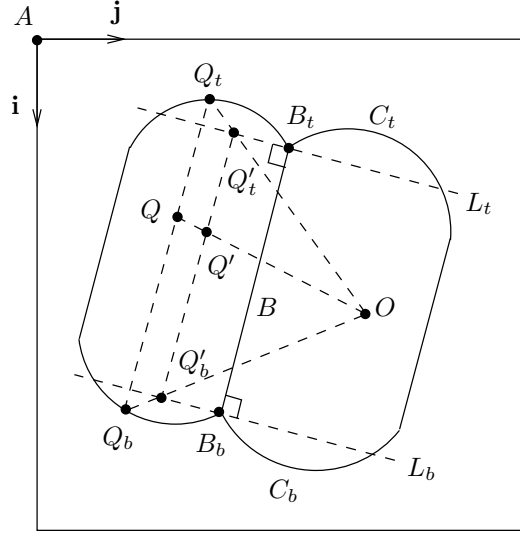


Fig. 4. Principle of the SFC method.

pixels Q'_b and Q'_t are defined without ambiguity (except if, exceptionnaly, O lies on L_b or on L_t). Consequently, system (9) becomes over-constrained and has an exact solution only if the line $(Q'_b Q'_t)$ is parallel to B . But it is even more significant to notice that, if the coordinates of O are unknown, the system is still well-constrained. Indeed, projecting (9) on an axis parallel to the binding, it comes easily:

$$z = -d \frac{\|\mathbf{B}_b - \mathbf{B}_t\|}{\|\mathbf{Q}_b - \mathbf{Q}_t\|}. \quad (10)$$

Under hypotheses H1-H2-H3, we propose, contrary to [8], an expression of z which is independent on the principal point.

Shape From Shading. The SFS method supposes that the 3D shape is regular enough, so that the outgoing unit normal $\mathbf{n}(P)$ is defined, without any ambiguity, at each 3D point P (*cf.* Figure 3). Recently, three groups of authors [14, 15, 11] have simultaneously expressed $\mathbf{n}(P)$ under the assumption of perspective projection:

$$\mathbf{n}(P) = \frac{(-h(i, j) \partial_i u(i, j) \quad -h(i, j) \partial_j u(i, j) \quad 1)^T}{\sqrt{h(i, j)^2 \|\nabla u(i, j)\|^2 + 1}}, \quad (11)$$

where $h(i, j) = f/v(i, j)$ and $v(i, j) = u(i, j) + i \partial_i u(i, j) + j \partial_j u(i, j)$. Note that this supposes that $(A\mathbf{i}j)$ is now orthonormal. The basic equation of SFS links the greylevel at a pixel Q to the normal $\mathbf{n}(P)$ at its conjugate point, but this is possible only if the illumination of the scene and the reflectance of the

surface are known at each point P . Otherwise, SFS would be ill-posed. The most classical assumptions are the following: the scene is lighted by a uniform parallel frontal beam (assumption H4); the surface is Lambertian (assumption H5). In order to satisfy H4, we light the scene with the annular flash described above. The second hypothesis (H5) is more difficult to control. Indeed, it does not hold for glazed paper. Moreover, the reflectance is not totally known under the assumption H5, because another characteristic of the surface, the albedo ρ , must be known: ρ is equal to $(1, 1, 1)$ for non-inked white paper, to $(0, 0, 0)$ for black-inked paper, and can take all values in $[0, 1]^3$ which correspond to all possible colors. As a consequence, we will compute $\mathbf{n}(P)$ only for the non-inked points P . Under assumptions H4-H5, it has been shown in [14, 15, 11] that the perspective SFS problem can be expressed through a partial-differential equation of the first order, named ‘‘perspective eikonal equation’’. In [14, 15], this equation is directly solved with u as unknown. In [11], $\mathbf{n}(P)$ itself is considered as a new unknown, via two functions p and q such that:

$$\mathbf{n}(P) = \frac{(-p(i, j) \quad -q(i, j) \quad 1)^T}{\sqrt{p(i, j)^2 + q(i, j)^2 + 1}}. \quad (12)$$

It is shown in [11] that the perspective eikonal equation can be transformed into:

$$p(i, j)^2 + q(i, j)^2 = \frac{g_{\max}^2}{g(i, j)^2} - 1, \quad (13)$$

where $g(i, j)$ designates the greylevel at pixel (i, j) , and g_{\max} its maximal value. Equation (13) is ill-posed, since there are two unknowns $(p(i, j), q(i, j))$ at each pixel. With an eventual change of coordinate system, so that $(A\mathbf{i})$ becomes parallel to the binding B and $(A\mathbf{j})$ becomes parallel to L_b and L_t (recall that $(A\mathbf{ij})$ is now supposed to be orthonormal), and under hypotheses H1-H2, it is easy to state that $p(i, j) = 0$. Moreover, using the a priori knowledge on the convexity of each page, $q(i, j)$ can be computed, without any concave/convex ambiguity, at each pixel on the book. Then, the last stage consists in computing u from q , which is not so evident as it could appear. From (11) and (12), it is shown in [11] that:

$$\nabla u(i, j) = \frac{u(i, j) \quad (p(i, j) \quad q(i, j))^T}{f - ip(i, j) - jq(i, j)}, \quad (14)$$

which is another partial-differential equation. This equation is definitely simpler to solve than the perspective eikonal equation, as it is linear.

Basic Difference between SFC and SFS. There is a basic difference between the two methods which were described. Whereas the knowledge of any intrinsic parameter is not required for SFC, it is for SFS. On the one hand, the focal length f appears explicitly in Equation (14). On the other hand, we have supposed $(A\mathbf{ij})$ to be orthonormal and chosen its origin A at the principal point O . As the pixel coordinates (i, j) explicitly appear in (14), it is necessary to know the calibration matrix \mathbf{K} .

Flattening. The flattening consists, as already said, in two steps: unwarping and interpolation. We used the same unwarping method than that described in most of the papers dealing with cylindrical warping [10, 4, 8].

The second step is a difficult task. We tried three different methods: the Smythe’s algorithm [12], through the free software `xmorph`; the Delaunay triangulation which is implemented in `MATLAB`; and a hardware solution via `OpenGL`. Because it is faster and easier to deal with, we preferred the `OpenGL` solution.

2.3 Results

In order to validate our two methods of geometric correction, we chosed the two images shown on the left column of Figure 5. The first one (Figure 5a) is the photograph of a regular grid, while the second one is the left half of the photograph shown in Figure 1a.

The results on the first image are presented in Figures 5b (SFC correction) and 5c (SFS correction). These results are particularly interesting, because they prove that both methods are able to retrieve the Euclidian structure of the flat page, since the lines of the grids are quasi-rectilinear and equally spaced, without having used this information as a priori knowledge.

The results on the second image, which are presented in Figures 5b’ (SFC correction) and 5c’ (SFS correction), are also quite satisfactory. A fast comparison between these two last images shows that SFC carries out a slightly better correction than SFS. This is due to the fact that the hypothesis specific to SFC (H3: the flattened page is supposed to be rectangular) is easier to guarantee than the two hypotheses specific to SFS (H4: parallel, uniform and frontal lighting; H5: Lambertian surface). In particular, hypothesis H4 is partially false near the binding, because of secondary reflections (in [9], the effects of secondary reflections are partially taken into account).

3 Photometric correction

3.1 Previous Work

Once they are geometric corrected, the images have still photometric defects, since the non-inked paper is not uniformly bright (*cf.* Figures 5b, 5c, 5b’ and 5c’). In order to correct these defects, different techniques have been proposed, but most of them are rather naive: either they threshold the image [1, 7], or an interpolation method is applied to simulate a “shading image” [3], or even no correction is done [6, 4, 8, 2]. Some authors [16, 9] simulate a shading image using Equation (13) and the knowledge of the shape obtained from the stage of geometric correction (thereafter, this simulation will be denoted SFS^{-1}). Since we know the document shape, as well as the surface reflectance and the lighting of the scene (hypotheses H4-H5), it could be interesting to calculate the shading image of a non-inked document having the same shape. Figure 7 shows how this shading image is used in our complete processing chain. Note that the photograph is first photometric corrected and then flattened.

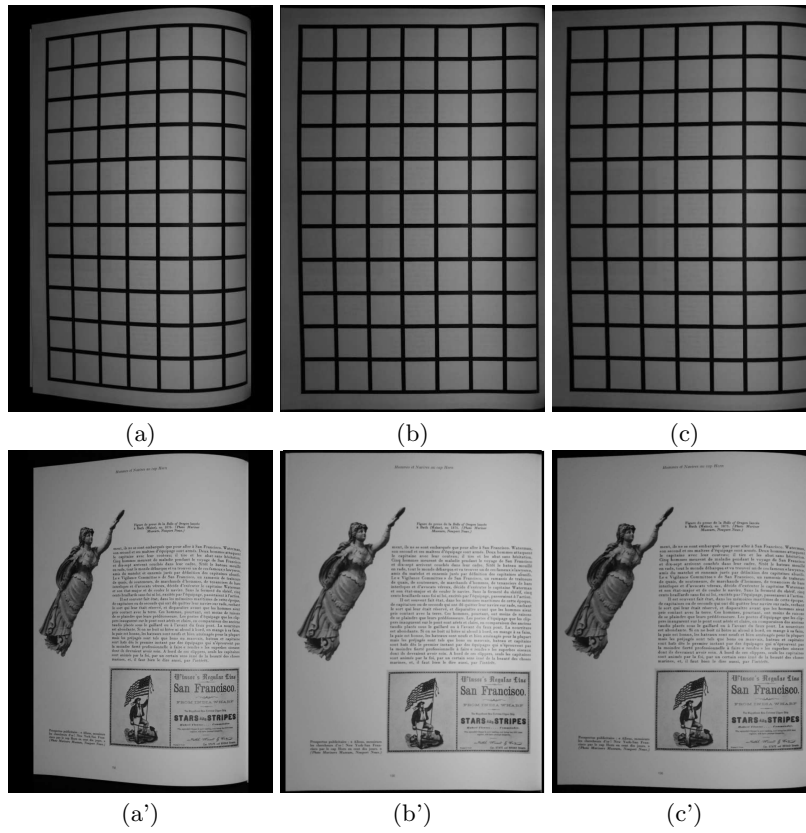


Fig. 5. (a-a') Original photographs and geometric corrected images using (b-b') SFC or (c-c') SFS.

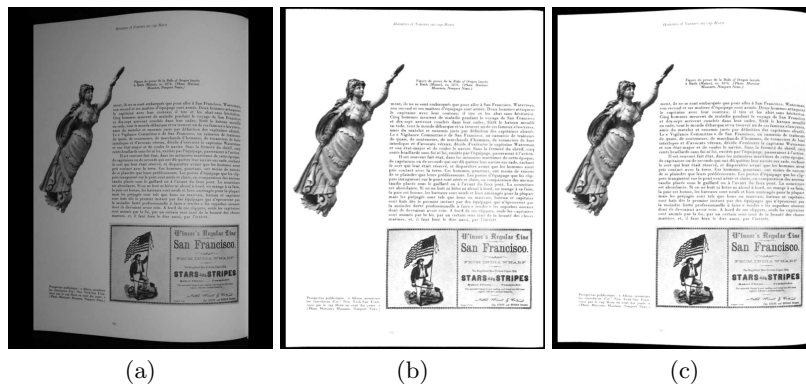


Fig. 6. (a) Original photograph and final corrected images after geometric correction using (b) SFC or (c) SFS, and photometric correction using SFS^{-1} .

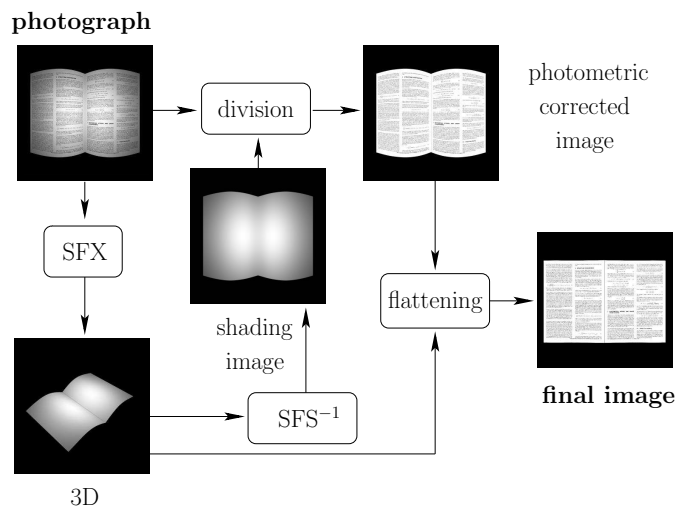


Fig. 7. Complete processing chain.

3.2 Results

The final corrected images of the photograph of Figure 6a are presented in Figures 6b and 6c. As can be seen, the backgrounds of the text (*i.e.*, the non-inked areas) look uniformly white, whereas all the text areas and pictures have recovered their original appearance. Finally, these two images look nearly the same.

4 Discussion

4.1 Readability of the Text

Figures 8 show three sub-images extracted from Figures 6a, 6b and 6c, corresponding to the same zone of text. In order to validate these results more rigorously, we ran the free OCR software `gocr`¹ on these three sub-images and on the scanned image. The results, which are reported in Table 1, show that both corrections enable the OCR to decide more often and in a more reliable way than on the photograph.

4.2 Limits of the Two Methods

As already said, the two methods of reconstruction produce relatively similar results. However, both methods cannot work on the same images.

¹ <http://jocr.sourceforge.net/>

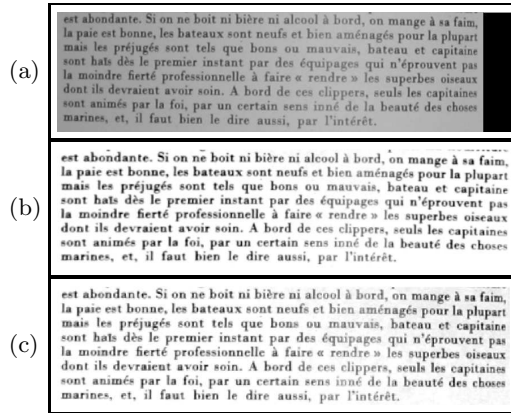


Fig. 8. Zooms (a) on the photograph of Figure 6a, (b) on the SFC corrected image of Figure 6b and (c) on the SFS corrected image of Figure 6c.

	(a)	(b)	(c)	(d)
success	2 %	61 %	55 %	92 %
failure	70 %	24 %	28 %	6 %
abstention	28 %	15 %	17 %	2 %

Table 1. OCR results on the same zone of text of the four following images: (a) photograph of the warped document; (b) SFC corrected image; (c) SFS corrected image; (d) scanned image of the flat document.

For example, the photograph shown in Figure 9a cannot be corrected using SFC, since no contour is visible, whereas SFS gives the good result shown in Figure 9c. On the other hand, SFS cannot work on the photographs shown in Figures 9a' and 9a'': all the document is inked in the case of Figure 9a'. Which means that the albedo is unknown; the lighting is not controlled in the case of Figure 9a'', where the annular flash has not been used. Figures 9b' and 9b'' show the good results obtained for the same photographs using SFC. Note that no photometric correction has been applied to these two last images, whereas this would have been possible using SFS^{-1} , once the shape is known. Nevertheless, such a correction would have been destined to failure for each of these images, because one of the SFS hypotheses (H5 for 9a' and H4 for 9a'') obviously does not hold. Other methods of photometric correction perhaps would be more appropriate, as for instance that described in [3] in the case of the image of Figure 9a''.



Fig. 9. (a) Photograph without visible contour; (b) SFC does not work; (c) SFS corrected image; (a') photograph with visible contour but unknown albedo; (b') SFC corrected image; (c') SFS does not work; (a'') photograph taken without control on the lighting; (b'') SFC corrected image; (c'') SFS does not work.

4.3 Relaxation of the Hypotheses

We already noted a significant disymetry between SFC and SFS: whereas SFC can be used with an uncalibrated camera, this is impossible for SFS. In order to highlight this disymetry, we took two photographs, represented in Figures 10a and 10a', using an uncalibrated consumer camera (Nikon Coolpix 775) without using an optical bench. Consequently, hypothesis H1 (fronto-parallelism) and the knowledge of the principal point coordinates are lost. Nevertheless, the results presented in Figures 10b and 10b' are of very good quality.

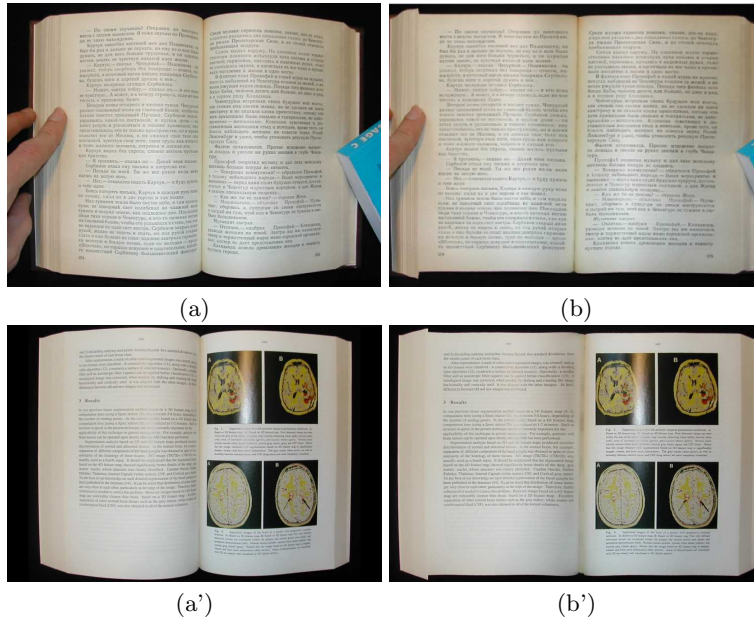


Fig. 10. (a-a') Photographs taken with an uncalibrated consumer camera and (b-b') geometric corrected images using SFC.

5 Conclusion and Perspectives

In this paper, we have proposed to use two SFX methods that take perspective into account, in order to simulate the flattening of a cylindrically-warped document from one photograph. The performances of the resulting algorithms have been illustrated on a practical application with real images.

As a perspective, we must now address the problem of simulating the flattening of non-cylindrical documents. This will probably require the fusion of SFC and SFS, since each method will become ill-posed for such shapes.

References

1. Zhang, Z., Tan, C.L.: Recovery of Distorted Document Images from Bound Volumes. In: Proc. of the International Conference on Document Analysis and Recognition. (2001) 429–433
2. Brown, M.S., Seales, W.B.: Image Restoration of Arbitrarily Warped Documents. IEEE Trans. PAMI **26** (2004) 1295–1306
3. Tsoi, Y.C., Brown, M.S.: Geometric and Shading Correction for Images of Printed Materials: A Unified Approach Using Boundary. In: Proc. of CVPR. Volume 1. (2004) 240–246
4. Yamashita, A., Kawarago, A., Kaneko, T., Miura, K.T.: Shape Reconstruction and Image Restoration for Non-Flat Surfaces of Documents with a Stereo Vision System. In: Proc. of ICPR'04. Volume 1. (2004) 482–485
5. Cho, S.I., Saito, H., Ozawa, S.: A Divide-and-conquer Strategy In Recovering Shape Of Book Surface From Shading. In: Proc. of ICIAP'97. Volume 2. (1997) 262–269
6. Doncescu, A., Bouju, A., Quillet, V.: Former books digital processing: image warping. In: Proc. of the Workshop on Document Image Analysis. (1997) 5–9
7. Cao, H., Ding, X., Liu, C.: A Cylindrical Surface Model to Rectify the Bound Document Image. In: Proc. of ICCV'03. Volume 1. (2003) 228–233
8. Kashimura, M., Nakajima, T., Onda, N., Saito, H., Ozawa, S.: Practical Introduction of Image Processing Technology to Digital Archiving of Rare Books. In: Proc. of the Int. Conf. on Signal Processing Application Technology. (1999)
9. Wada, T., Ukida, H., Matsuyama, T.: Shape from Shading with Interreflections under Proximal Light Source: 3D shape Reconstruction of Unfolded Book Surface from a Scanner Image. In: Proc. of ICCV'95. (1995) 66–71
10. Zhang, Z., Tan, C.L., Fan, L.: Restoration of Curved Document Images through 3D Shape Modeling. In: Proc. of CVPR. (2004) 10–15
11. Courteille, F., Crouzil, A., Durou, J.D., Gurdjos, P.: Towards shape from shading under realistic photographic conditions. In: Proc. of ICPR'04. Volume 2. (2004) 277–280
12. Smythe, D.B.: A Two-Pass Mesh Warping Algorithm for Object Transformation and Image Interpolation. Technical Memo 1030, Industrial Light and Magic, Computer Graphics Department, Lucasfilm Ltd. (1990)
13. Hartley, R.L., Zisserman, A.: Multiple View Geometry in Computer Vision. second edn. Cambridge University Press (2003)
14. Prados, E., Faugeras, O.: “Perspective Shape from Shading” and Viscosity Solutions. In: Proc. of ICCV'03. Volume 2. (2003) 826–831
15. Tankus, A., Sochen, N., Yeshurun, Y.: A New Perspective [on] Shape-from-Shading. In: Proc. of ICCV'03. Volume 2. (2003) 862–869
16. Zhang, Z., Tan, C.L., Fan, L.: Estimation of 3D Shape of Warped Document Surface for Image Restoration. In: Proc. of ICPR'04. Volume 1. (2004) 486–489